

ACOUSTIC SIGNATURES ACCOMPANYING
LOW-VELOCITY WATER ENTRY

Brian Douglas Uber

NAVAL POSTGRADUATE SCHOOL

Monterey, California



THESIS

ACOUSTIC SIGNATURES
ACCOMPANYING LOW-VELOCITY WATER ENTRY

by

Brian Douglas Uber

Robert Joseph Fegan, Jr.

Thesis Advisor:

J. V. Sanders

December 1973

Approved for public release; distribution unlimited.

T158168

Acoustic Signatures
Accompanying Low-Velocity Water Entry

by

Brian Douglas Uber
Lieutenant, United States Navy
B.S., United States Naval Academy, 1965

and

Robert Joseph Fegan, Jr.
Lieutenant Commander, United States Navy
B.S., United States Naval Academy, 1964

Submitted in partial fulfillment of the
requirements for the degree of

MASTER OF SCIENCE IN ENGINEERING ACOUSTICS

from the

NAVAL POSTGRADUATE SCHOOL
December 1973

Thes
u 125
c. 1

ABSTRACT

Solid metal spheres, simple missile-like shapes, and a bowling ball were dropped from varying heights below 4 m into a water-filled anechoic tank and the resulting acoustic signatures were recorded and analyzed. In addition, the hydrodynamics of the drops were recorded on movie film for correlation with the acoustic signature.

The oscillation of the air-filled cavity behind the bodies after impact was found to produce the most predominant aspect of the acoustic signature and the resultant frequency of these oscillations was dependent upon the impacting kinetic energy and shape of the body. Other signal characteristics investigated were total acoustic energy, peak acoustic pressure, and decay rate but correlation with the parameters of the bodies was not obvious.

TABLE OF CONTENTS

I.	INTRODUCTION-----	5
II.	APPARATUS-----	9
III.	EXPERIMENTAL PROCEDURE-----	18
IV.	PRESENTATION OF DATA AND RESULTS-----	24
V.	CONCLUSIONS AND APPLICATIONS-----	42
	APPENDIX A Summary of Data-----	44
	BIBLIOGRAPHY-----	47
	INITIAL DISTRIBUTION LIST-----	49
	FORM DD 1473-----	50

LIST OF FIGURES

1.	Data Collection Equipment-----	12
2.	Schematic Diagram of Audio Signal Monitoring and Recording System -----	14
3.	Typical Signature of Solid Metal Sphere Impacting Water Surface -----	26
4.	Representative Missilegram. Frequency vs. Time -----	27
5.	Representative Missilegram. Frequency vs. Relative Amplitude-----	28
6.	Representative Visicorder Signature-----	29
7.	Dominant Frequency vs. Impacting Kinetic Energy -----	31
8.	Dominant Frequency vs. \log_{10} (Impacting Kinetic Energy) -----	32
9.	Missile-Like Shapes. Dominant Frequency vs. Impacting Kinetic Energy -----	34
10.	Metal Spheres. Acoustic Pressure vs. Impacting Kinetic Energy-----	36
11.	Bowling Ball. Acoustic Pressure vs. Impacting Kinetic Energy-----	37
12.	Metal Spheres. Acoustic Energy Flux Density vs. Impacting Kinetic Energy -----	38
13.	Bowling Ball. Acoustic Energy Flux Density vs. Impacting Kinetic Energy -----	39
14.	Metal Spheres. Signal Decay Constant vs. Impacting Kinetic Energy-----	40
15.	Bowling Ball. Signal Decay Constant vs. Impacting Kinetic Energy-----	41

I. INTRODUCTION

Water entry refers to a sequence of events which accompany the passage of a body through the water-air interface. The sequence of events is commonly divided into the following phases: (1) shock wave phase in which a shock wave is generated and the body experiences the greatest forces, (2) flow-forming phase in which flow is generated in water that was initially at rest and the body experiences the greatest deceleration, (3) open-cavity phase in which the cavity generated by the body as it travels down through the water is open to the atmosphere, (4) closed-cavity phase in which the cavity closes, (5) collapsing-cavity phase in which the cavity size is decreasing due to increasing hydrostatic pressure, and (6) fully-wetted phase in which the cavity separates from the body and water covers the complete surface of the body [1].

Past interest and experimental work with water entry has been primarily concerned with the hydrodynamics and the behavior of a body as it enters water from the air. Areas of research have been concerned with the forces and torques on the entry body due to impact and movement through the water and the splash and cavity formation processes. Some correlation of the hydrodynamics with the frequency spectrum of the acoustic signal produced by the water entry has also been attempted.

The first published experimental results in this field were by Worthington. As a follow-on to his 1876 experiments to determine the forms assumed by liquid drops when they impacted on a horizontal plate [2], Worthington in 1882 investigated the forms of splashes made by drops of liquid and solid spheres impacting with a liquid surface [3]. Worthington and Cole repeated these experiments in 1895 and 1899, expanding the program to include the study of the effects of the surface conditions of the spheres and to record the splashes and the cavity using photography [4, 5].

Experiments by Minnaert in 1933 on air bubbles generated underwater resulted in an expression for the period of oscillation of a spherical bubble relating the potential energy of the bubble to the kinetic energy of the bubble in equilibrium. This expression reduces to a function in which the period is proportional to the radius of the bubble [6]. Franz generalized Minnaert's expression to apply to any bubble, spherical or non-spherical in shape, in which the radius is redefined as the volumetric-mean radius, or the radius of a sphere having the same volume as the bubble [7].

In 1948 May and Woodhull experimentally determined the drag coefficients of steel spheres entering water as functions of Reynolds and Froude numbers [8]. Further studies by May in 1951 and 1952 determined the effects of variations in the surface conditions of a sphere on the various phases of cavity formation which may accompany

water entry; he also studied the effects of the density and pressure of the atmosphere along with the velocity, size, and nose shape of a body [9, 10].

In 1948 and 1955 Richardson recorded on motion picture film the air cavity formed behind a body after it impacted upon the water and as it descended through the water. He made correlations between the hydrodynamics and the acoustic signature as recorded by microphone and hydrophone. Richardson also analyzed his data to determine the sources of the various frequencies in his acoustical recordings [11, 12].

Studies by Franz in 1955 and 1958 established formulation for determining frequency, sound pressure, and radiated sound energy that are generated during the flow establishment, body vibration, and cavity and bubble phases of the water entry of a body. Franz also conducted detailed frequency analyses and acoustic/hydrodynamic correlation of his data [7, 13].

The initial incentive for conducting this research was interest in the acoustics of low-velocity water entry, underwater travel, and water exit of a weapon-shaped body. The scope of interest was quickly narrowed to strictly water entry aspects, and in particular the following objectives were pursued: (1) to relate the source of predominant acoustic energy to some phase of hydrodynamic activity by correlating the recorded acoustic signal and the photographic record of the water entry, (2) to determine the frequency of the predominant portion of

the acoustic signal, (3) to determine the peak sound pressure and acoustic energy imparted to the water, and (4) to determine "modeling parameters" that would relate the characteristics of the impacting body to the acoustic signal.

II. APPARATUS

The apparatus and equipment utilized were far from state-of-the-art for this type of research due primarily to a lack of local facilities. Nevertheless they were adequate, and provided sufficiently accurate data to fulfill the goals of the project.

Procedural details will be treated in the next section, but basically all data was collected by dropping bodies into a water-filled tank, and recording the resultant acoustic signature on a tape recorder as the hydrodynamic action was recorded on motion picture film.

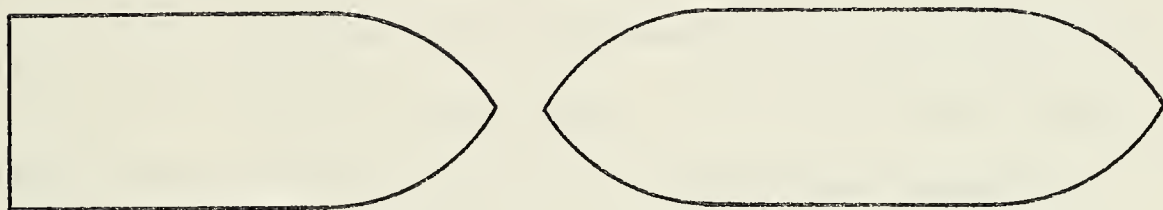
The tank used was one of two permanently installed in the floor of the basement of Spanagel Hall at the Naval Postgraduate School. Each tank measures approximately 24 ft by 6 ft with a water depth of 7 ft, and the inner surfaces are lined with a rough, rubber-base material several inches thick which exhibits anechoic properties at frequencies greater than 15 kHz. The frequencies of interest in this research were quite low (below 100 Hz) but reflections from the tank walls were not observed. Prior to each filming session, the water was filtered through the installed filter system and then allowed to settle for at least one day.

A majority of data was generated by dropping metal spheres into the tank from varying heights. All the spheres were painted

white to enhance underwater visibility. One set of spheres was aluminum, the other brass, and diameters for each set were 2.5, 3, 3.5, and 4 in.

A standard-size bowling ball weighing 15.8 lb was dropped into the water to generate high-energy data.

Also utilized for a small amount of data were two simple, missile-like shapes machined from round aluminum stock of 2.5 in. diameter. One was 7 in. long with one end flat and the other machined to a taper. The other shape was 9.5 in. long with both ends machined to a taper. The following is a sketch of the shapes:



For purposes of raising and suspending the bodies above the water prior to their drop, all spheres and shapes were fitted with a small metal eyelet to which was fastened a length of monofilament line. When a drop was made, the eyelet and line remained attached but this was considered to have negligible influence on the acoustical signature. Prior to a drop, each body was cleaned with a freon-base degreasing agent to eliminate any variation in surface conditions.

The rest of the drop mechanism was equally simple, consisting merely of a metal eyebolt clamped to an overhead beam above the

tank through which was passed the monofilament line. The line then led back down to floor level where it was controlled and released by hand. This rig was used for all drops except the bowling ball which was dropped by hand from a step ladder. For the missile-like shapes, a 5 ft length of aluminum pipe was used as a guide to ensure a near-vertical water entry. A long measuring rod was used to check the height above the water surface prior to each drop, the height being the controlling parameter for impact velocity.

The filming apparatus consisted of a movie camera and high-intensity lights contained within a specially constructed, submersible, wooden chamber with a built-in viewing window.

All filming was done with a Bolex Model 160, 8 mm movie camera using Kodak Ektachrome ASA 160 film. The fastest available frame rate of 36 sec^{-1} was employed and provided reasonably good time resolution. Camera lens-to-object distance was 1.5 m and the zoom-lens feature was used in the fully magnified position. The built-in light meter/electric eye was used in the automatic position.

Lighting was provided by two 1000 watt halogen-tungsten element photographic lights mounted directly above and below the camera so that essentially all light into the water was from behind the lens. The equipment within the submersible chamber is illustrated in Fig. 1.

Since the installed water tanks had no built-in features for underwater photography some provision had to be made for submerging the

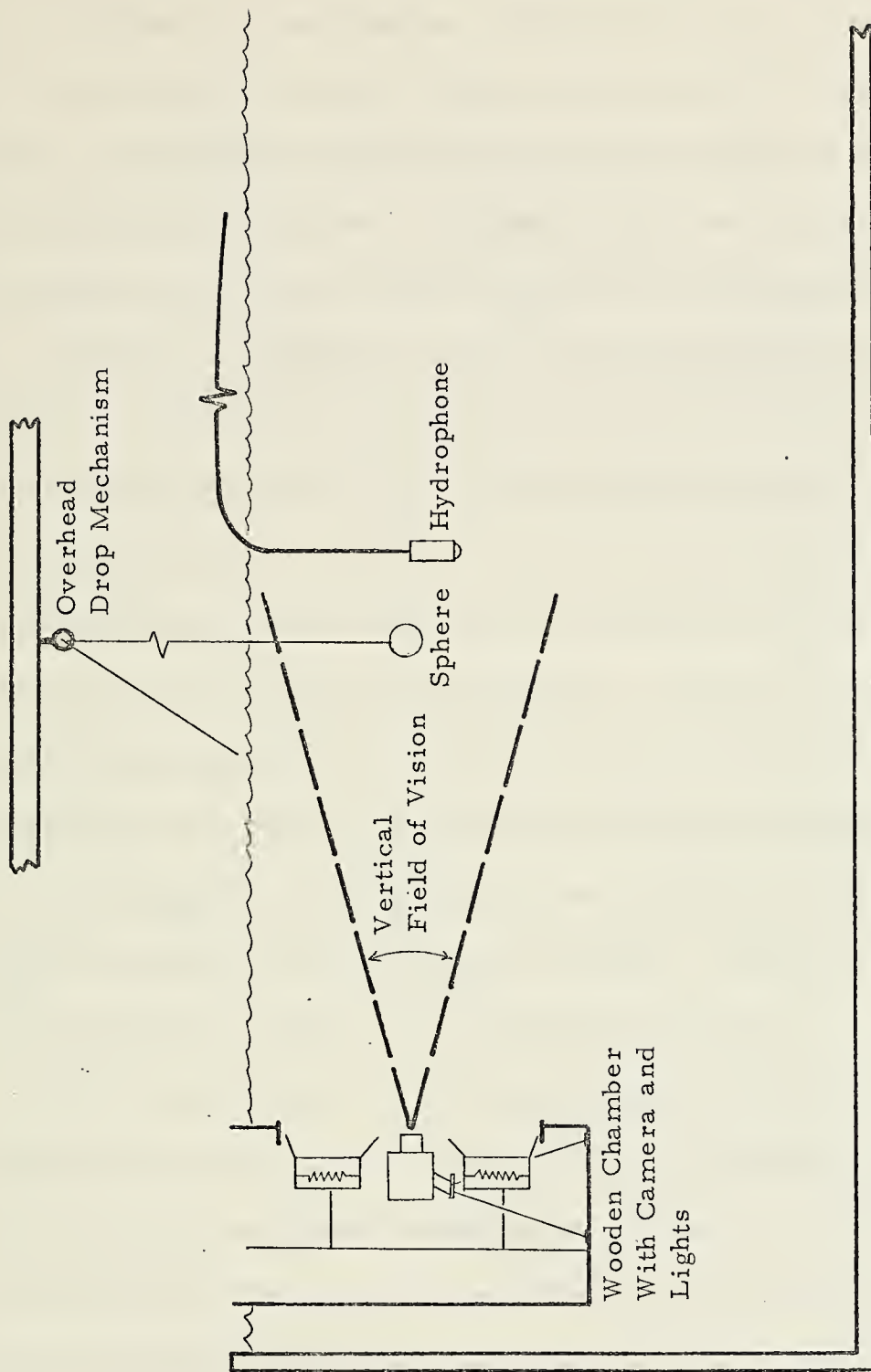


FIGURE 1. DATA COLLECTION EQUIPMENT

camera and lights. A very practical solution to the problem was the submersible, wooden chamber. The dimensions of the chamber were 2 ft by 2 ft, and 4 ft deep. This large size permitted all equipment to be mounted in the chamber and adjusted as necessary to provide the field of vision desired. Additionally there was enough room for a person to go into the chamber to adjust the equipment prior to filming.

Figure 2 is a schematic of the audio recording setup. The hydrophone used for receiving all acoustical information was an Atlantic Research Corporation LC-32. This particular unit was chosen primarily because it exhibits a constant free-field voltage sensitivity in the frequency range of interest (approximately 30-1000 Hz) and because of its portability and availability. For most of the drops, a hydrophone position of 50 cm below the water surface and 30 cm lateral distance from the drop path was found to be suitable.

The signal from the hydrophone was amplified by a Burr-Brown Model 100 battery-power amplifier by 20 dB. This type amplifier was chosen as a means of reducing 60 Hz interference.

The signal was then recorded on magnetic tape by a Precision Instrument tape recorder, Model PI-6200 in the frequency modulation record/reproduce mode. A tape speed of 3.75 in./sec and center frequency of 5 kHz provided a response of ± 1 dB from dc to 1 kHz. During playback, the built-in output filter of 100 Hz was selected to eliminate signal components not of interest in this research.

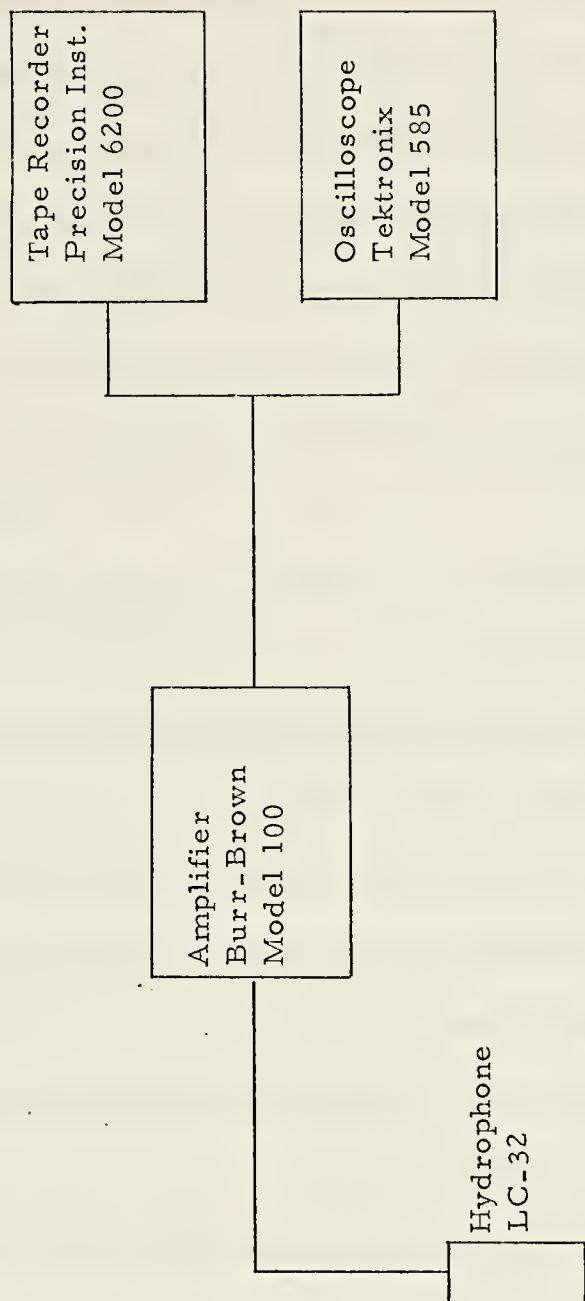


FIGURE 2. SCHEMATIC DIAGRAM OF AUDIO
SIGNAL MONITORING AND RECORDING SYSTEM

Several different pieces of signal analysis equipment were utilized and their basic capabilities will be summarized here. In the next section, Experimental Procedure, their actual application and output interpretation will be explained in detail.

A Tektronix Type 565 Oscilloscope was used to monitor hydrophone output in order to view the general signature characteristics, primarily to determine if sufficient signal strength existed to permit meaningful reproduction from the tape. Polaroid scope photographs were taken of some signatures to provide a permanent record for later analysis.

During early stages of analysis, a Kay Electric Company Missilyzer was employed to process the recorded signatures. The Missilyzer is an audio spectrograph which produces a permanent visual record of an input waveform. The graphic recording is referred to as a Missilegram, or simply "gram". Several different analyses of recorded data are possible with the Missilyzer; one relates frequency and intensity to time and another relates intensity to frequency at a chosen instant of time. In normal operation a gram portrays frequency along a vertical displacement of 4 in. and time along a 12.5 in. horizontal displacement.

To analyze a signal on the Missilyzer, it is first recorded internally, after which it is reproduced repeatedly at high speed. On each repetition the signal is scanned by a band-pass filter, which

is effectively shifted slightly in frequency with each repetition. The output of the analyzing filter is then recorded on dry facsimile paper. The recording stylus shifts gradually along the frequency scale in step with the scanning filter. Variations in voltage at the output of the filter appear on the gram as light or dark areas, with the higher voltage levels showing in the darker regions [14].

Considered to be of greatest benefit for accurate signal analysis was a Honeywell Visicorder Model 1508B. The principle of operation is for a narrow, high intensity light beam to be deflected laterally in proportion to changes in signal amplitude as the light-sensitive recording paper passes beneath the beam. Paper speeds up to 80 in/sec are available and thus it was possible to examine in great detail the nature of each signature.

A real-time spectrum analyzer, the Model 1510 Spectrameter, was available for several hours during a demonstration visit by a representative of EMR Telemetry, Weston Instruments, Inc. A number of signals previously analyzed on the Visicorder were processed by this equipment and comparison of results was quite favorable: most signals were within ± 1 Hz on the two different equipment. Of course the Spectrameter has many capabilities not available in the equipments previously discussed, and would have been of great value to this research in terms of time saved and accuracy of results. Spectrum analysis is accomplished by a built-in digital computer which

performs a Fourier transform on the signal contained in memory. As well as spectrum measurements, any transient signal (such as those encountered in this research) can be captured and displayed in the time domain before it is transformed into the frequency domain. Of particular application to this type of research would be this instrument's ability to digitally present frequency and spectrum level information [15].

Another method of analysis considered was that of digitizing the recorded signals and processing them through a Fast Fourier Transform Analysis Program available for the COMCOR 5000 computer. However, as it turned out, the signals of interest were of such short duration that a frequency accuracy on the order of ± 10 Hz was the best that could be obtained and this was considered unacceptable.

In summary, a number of methods of signal analysis were considered and tried and the best equipment available locally in terms of output clarity and accuracy was the Visicorder. Examples of the graphical outputs from the various equipments are included in the next section, Experimental Procedure.

III. EXPERIMENTAL PROCEDURE

Data collection procedures for this research involved several coordinated phases and many weeks of trial and error were required to perfect and simplify these various phases to a degree that would produce reliable data. This particular type of experiment had never been attempted previously at the Naval Postgraduate School and many problem areas, such as water clarity, underwater lighting, proper camera and hydrophone distances, and signal amplification, were encountered.

Once the procedures were perfected and the various problem areas were accounted for as best as possible, the preparations for a typical data run were as follows:

1. The tape recorder was calibrated in accordance with the instruction manual [16].
2. Equipment was set up as in Figs. 1 and 2.
3. Oscilloscope amplitude and time scales were selected and the proper trigger level was set.
4. The oscilloscope camera was adjusted.
5. The lights and camera were adjusted, and proper camera settings were made.

After these preliminary steps, it was time to record data and the following sequence of events took place:

6. The lights were turned on to illuminate the underwater drop zone.
7. The body to be dropped and raised to a predetermined height and steadied.
8. The tape recorder was started.
9. The movie camera was started.
10. The Polaroid camera shutter was opened.
11. The shape was released.
12. After impact, the Polaroid camera shutter was closed.
13. Approximately 10 sec after impact, the tape recorder and movie camera were turned off.
14. The camera lights were turned off.

The above procedures generated one datum. With subsequent changes in drop height or body, the procedures were repeated to generate an additional datum. After several sessions of recording data in this manner, a familiarity with signature and cavity formation characteristics was gained, and the scope photography and movie filming phases were eliminated to simplify the procedure.

After a set of data was recorded on film and tape, it was available for many forms of analysis. The primary purpose of the filming was to obtain a visual record of the hydrodynamic action for correlation with the audio-signature characteristics.

The first step in this comparison procedure was to analyze the oscilloscope photographs. It was assumed that the shock wave

produced at the instant of impact triggered the scope so that the signature could be subdivided along the time axis by starting at the time of impact and marking every 27.7 msec, which corresponds to a movie frame rate of 36 sec^{-1} . Next the movie film of the same drop was examined by manually feeding the film through a standard 8 mm projector and observing the impact and the cavity formation process. The actual impact of the sphere with the water surface was detectable on the film, and the frame in which it occurred then became time zero for comparison to the signatures.

Every signature possessed several cycles of a damped sinusoidal waveform having significantly greater amplitude than the remainder of the signature. The hydrodynamic source of this portion of the signature appeared to be oscillations of the underwater air cavity after it had reached maximum volume; this observation will be discussed further in the next section.

A significant amount of data analysis effort was directed at determining the frequency of this damped sinusoid, as well as measuring peak pressures and calculating the acoustic energy of the portion of the waveform of interest.

As indicated in the previous section, the Missilyzer was utilized extensively during the early stages of data analysis. A given signature was recorded on the Missilyzer from the tape recorder and then analyzed in the various manners. The 15-1500 Hz frequency

band was used initially to produce the frequency vs time plot and it soon became apparent after analysis of several signatures that all frequencies of significant amplitudes were below 100 Hz. In addition, a noticeable spike or darkening of the paper in one region of frequency occurred on most grams. This spike corresponds to the predominant frequency indicated earlier. This spike covered a band of frequencies on the order of 10-15 Hz and usage of the sectioning feature of the Missilyzer was inconclusive in attempting to evaluate the precise frequency. For this reason, the use of the Missilyzer was terminated, and more precise forms of frequency analysis were sought.

The oscilloscope photographs were one means of examining the actual signature waveform and calculating the characteristic frequency. For the waveform segment of interest, frequency calculation was quite simple: some number of cycles was counted and the elapsed time was measured. From these two values, it follows that:

$$f = 1/t = 1/(T/n) = n/T$$

where n = number of cycles counted, and

T = elapsed time in seconds for these n cycles.

The inherently small size of the oscilloscope photographs limited the accuracy of information derived from them and for this reason the Visicorder was brought into use. The waveforms reproduced by the Visicorder were, of course, identical to the oscilloscope photos but were of a much greater physical size. The paper is 8 in.

wide, and the high paper speeds permitted "stretching" the signal to suitable proportions for analysis. Frequency determination procedures were identical to those employed for the oscilloscope photos.

In addition to frequency analysis, the Visicorder provided the peak signal amplitude and decay constant of the signal. For each of the drops using the metal spheres and the bowling ball, the following steps were taken:

1. The natural logarithm of the peak positive voltage in each cycle was plotted against time and a straight line fit was made with 4 or more successive points actually lying on the line.
2. The decay constant of the signal was determined from the slope of the straight line.
3. The peak positive voltage of the first cycle was corrected, if necessary, to a value consistent with the straight line.
4. The extrapolated value of the signal voltage at the time that the first cycle started was determined from the straight line.
5. Since a 20 dB gain amplifier was used, the voltage at the hydrophone was one-tenth of the voltage of the recorded signal.
6. The free-field, plane-wave pressure, P , at the hydrophone was determined from:

$$M = 20 \log E/P \text{ (dB re 1 volt/ } \mu\text{bar)}$$

where M is the free-field voltage sensitivity of the LC-32 hydrophone, -103 dB re 1 volt/ μ bar, and E is the open circuit output voltage of the hydrophone; this yields the expression:

$$P = E/7.09 \times 10^{-6} \text{ (} \mu\text{bar)}.$$

7. The energy flux density of the signal was determined from the expression:

$$E = 1/\rho c \int_0^{\infty} p^2(t) dt$$

where ρc is the characteristic impedance of the water, and $p^2(t) = P^2 e^{-2t/\gamma} \sin \omega t$

where P is the free-field plane wave pressure as determined by using the value of signal voltage from step (4) and step (6), γ is the decay constant as determined in step (2), and ω is the frequency of the signal.

IV. PRESENTATION OF DATA AND RESULTS

Analysis of the film of the drops of the metal spheres indicated that the open-cavity and closed-cavity phases of water entry were the phases of significance in forming the acoustic signature. The shock-wave phase was not recorded either acoustically or cinematically due to its short duration. The shock-wave phase exists only while there is supersonic flow in the water; its duration is equal to the time during which the rate of introduction of the shape into the water is supersonic. For a sphere, the duration of supersonic flow is [13]:

$$t = rU_o/2c^2$$

where r = radius of the sphere,

U_o = impact velocity of the sphere, and

c = speed of sound in water.

The greatest duration of a shock-wave phase for this research was 99.3 nsec which would be a pulse having essentially all frequencies. The collapsing-cavity phase was recorded on film but it was considered to be an integral part of the closed-cavity phase in that the cavity did not detach itself from the surface and, when it vented to the atmosphere, it collapsed very rapidly. The fully-wetted phase was not recorded on film as it occurred out of the field-of-vision of the camera.

From analysis of the acoustic signature and comparison with the film, the significant features of the acoustical signal were assumed to be a result of the surface closure and the subsequent volume pulsations of the cavity. Surface closure occurs when the splash "domes over" and seals the cavity from the atmosphere [1]. Figure 3 is a reproduction of a typical signature generated by water entry of a metal sphere, and is annotated to point out the hydrodynamic activity associated with prominent features in the signature.

Figures 4 and 5 are representative grams from the Missilyzer. Figure 4 is a presentation of signal frequencies and relative amplitudes vs time. The "spike" at approximately 37 Hz, 0.25 sec after impact, is the signature of interest. Absolute signal amplitudes cannot be determined; their relative values of each other are indicated by the darkness of presentation. Figure 5 is a series of sections from the spike region of Fig. 5, each section being at a discrete time. The presentation is frequency vs relative amplitude. Figure 6 is a representative signature from the Visicorder, presenting the signal waveform vs time. Frequencies are determinable to within ± 1 Hz and signal amplitudes to within ± 5 mv.

By direct measurement, calculation, analysis, or a combination of same, the following data was available from any drop:

1. Size, shape, and mass of the body dropped.
2. Impact velocity of the body.

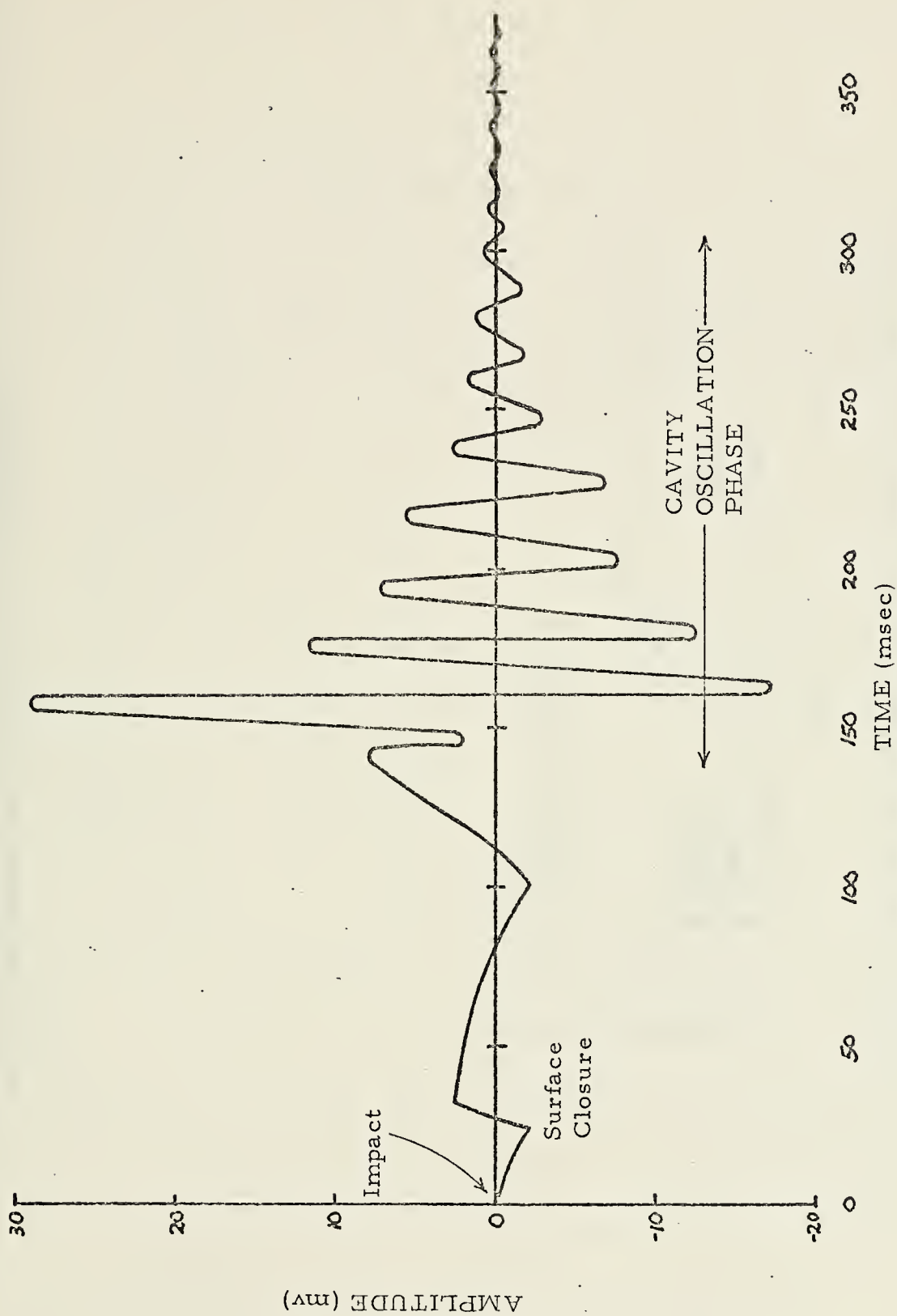


FIGURE 3. TYPICAL SIGNAL OF SOLID METAL SPHERE
IMPACTING WATER SURFACE

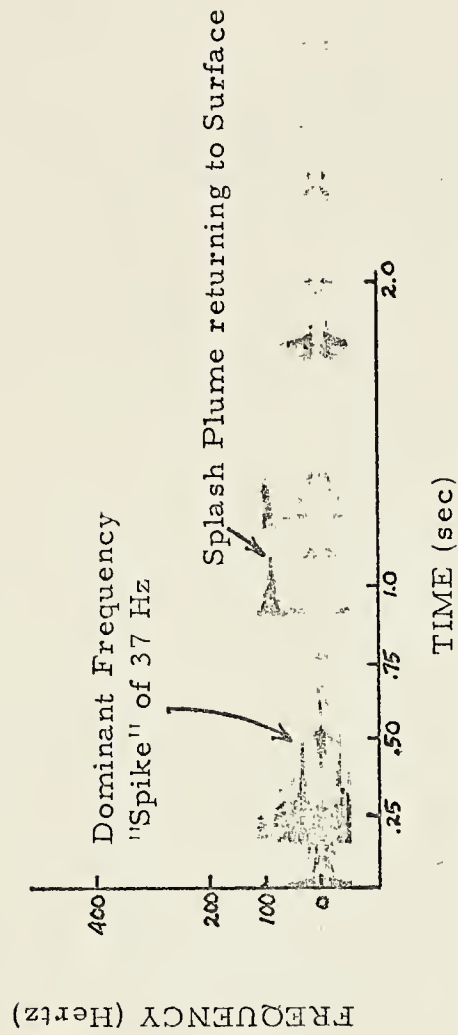


FIGURE 4. REPRESENTATIVE MISSILEGRAM.
FREQUENCY vs. TIME

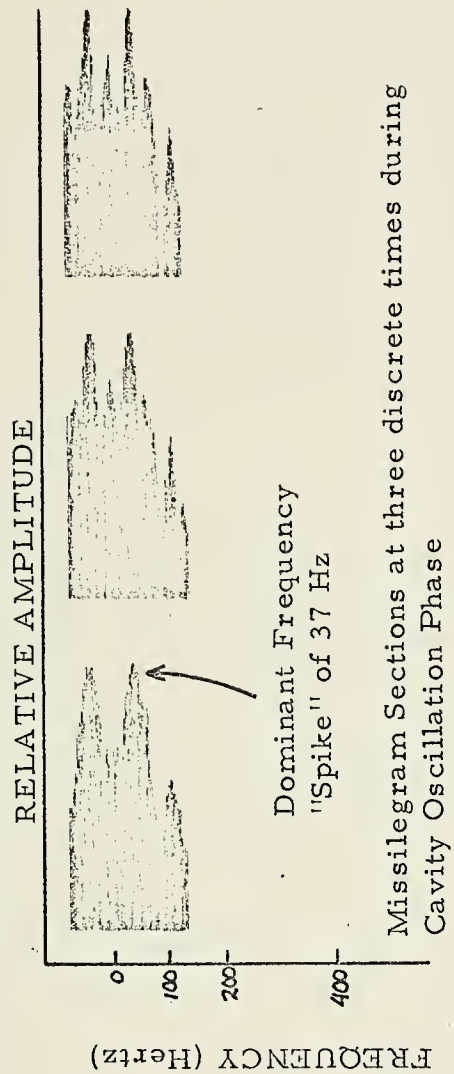


FIGURE 5. REPRESENTATIVE MISSILEGRAM.
FREQUENCY vs. RELATIVE AMPLITUDE

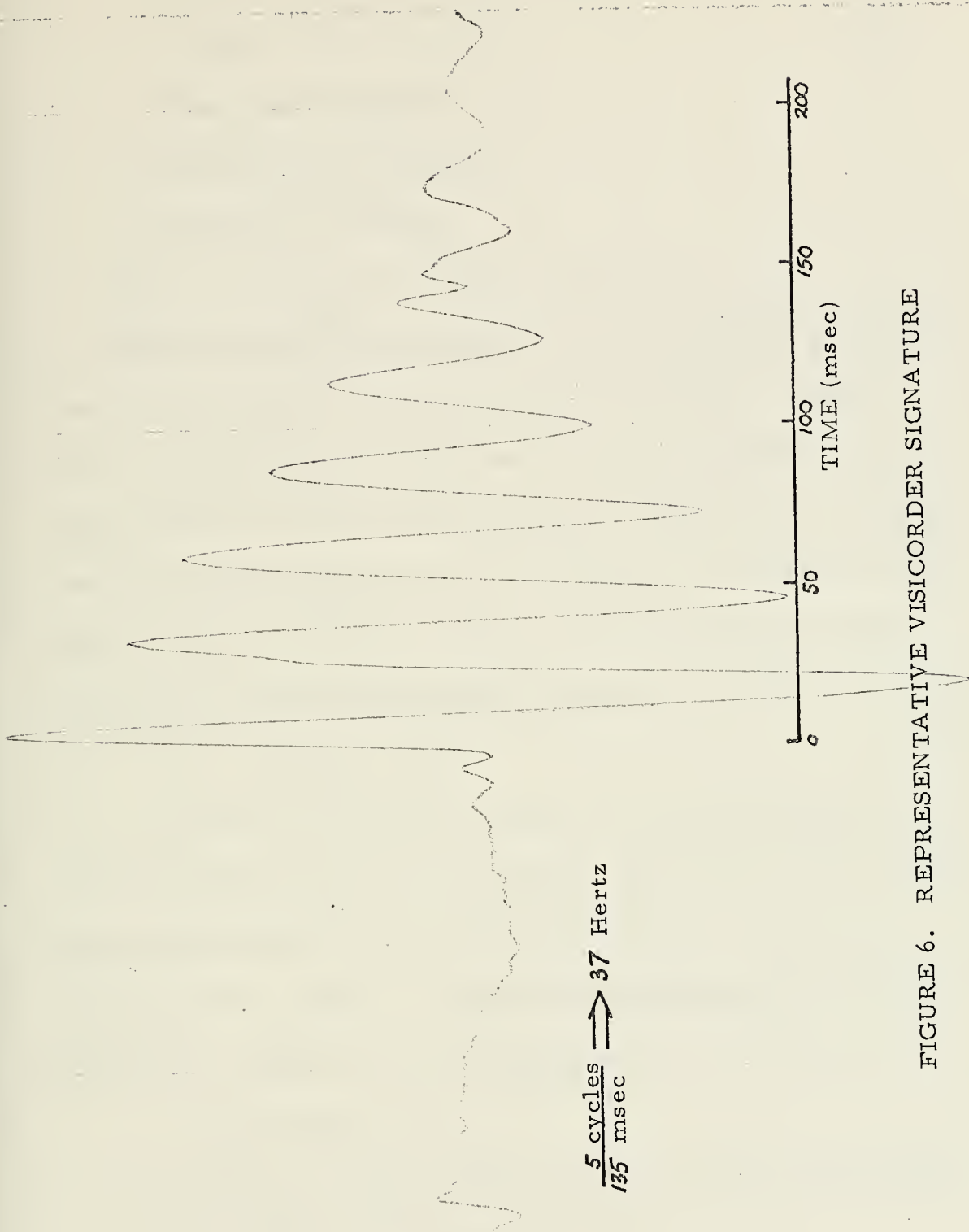


FIGURE 6. REPRESENTATIVE VISICORDER SIGNATURE

3. Kinetic energy of the body at impact.
4. Dominant signal frequency.
5. Peak signal amplitude.
6. Signal energy flux density.
7. Signal decay constant.

Figures 7 through 15 are plots of the results.

Figure 7 presents the dominant signal frequency vs the kinetic energy of the body at impact, and Fig. 8 the dominant signal frequency vs the logarithm of the kinetic energy of the body at impact. These plots represent the most significant results of this research and indicate that the dominant signal frequency is a function of the kinetic energy of the body at impact. An expression for the frequency in Hz as a function of kinetic energy is:

$$f = - 0.2 \log E + 79$$

where E is the kinetic energy of the impacting body in J.

As previously discussed, the principal acoustic source of the signal appeared to be the volume pulsations of the cavity. There is an expression that relates the frequency of oscillation of a spherical bubble to its radius [13]. This expression is:

$$f = (3 \gamma P_o / \rho)^{1/2} / 2 a$$

where γ = ratio of specific heats of the gas in the bubble,

P_o = environmental pressure,

ρ = density of water, and

a = radius of the bubble.

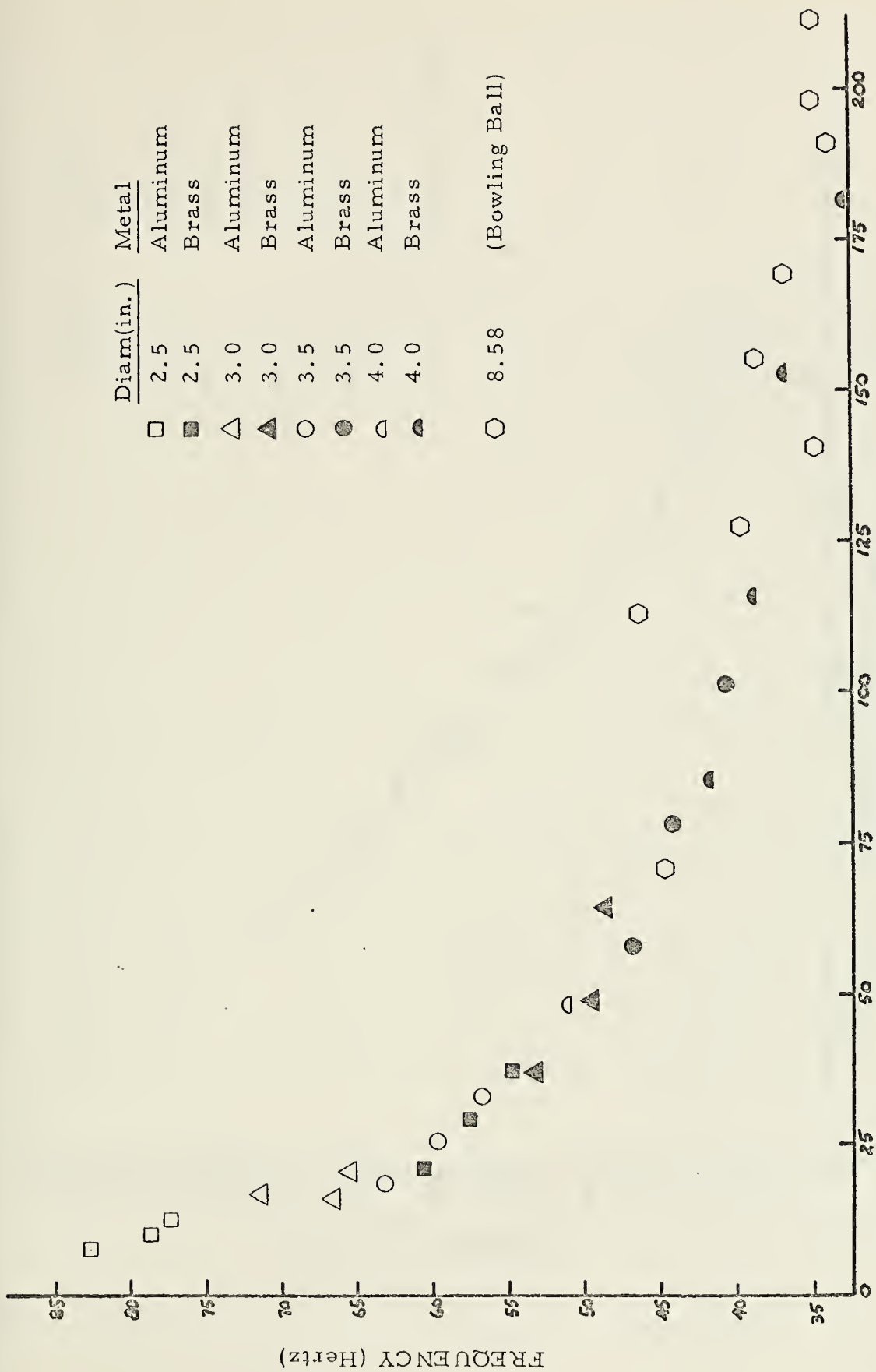


FIGURE 7. DOMINANT FREQUENCY vs. IMPACTING KINETIC ENERGY

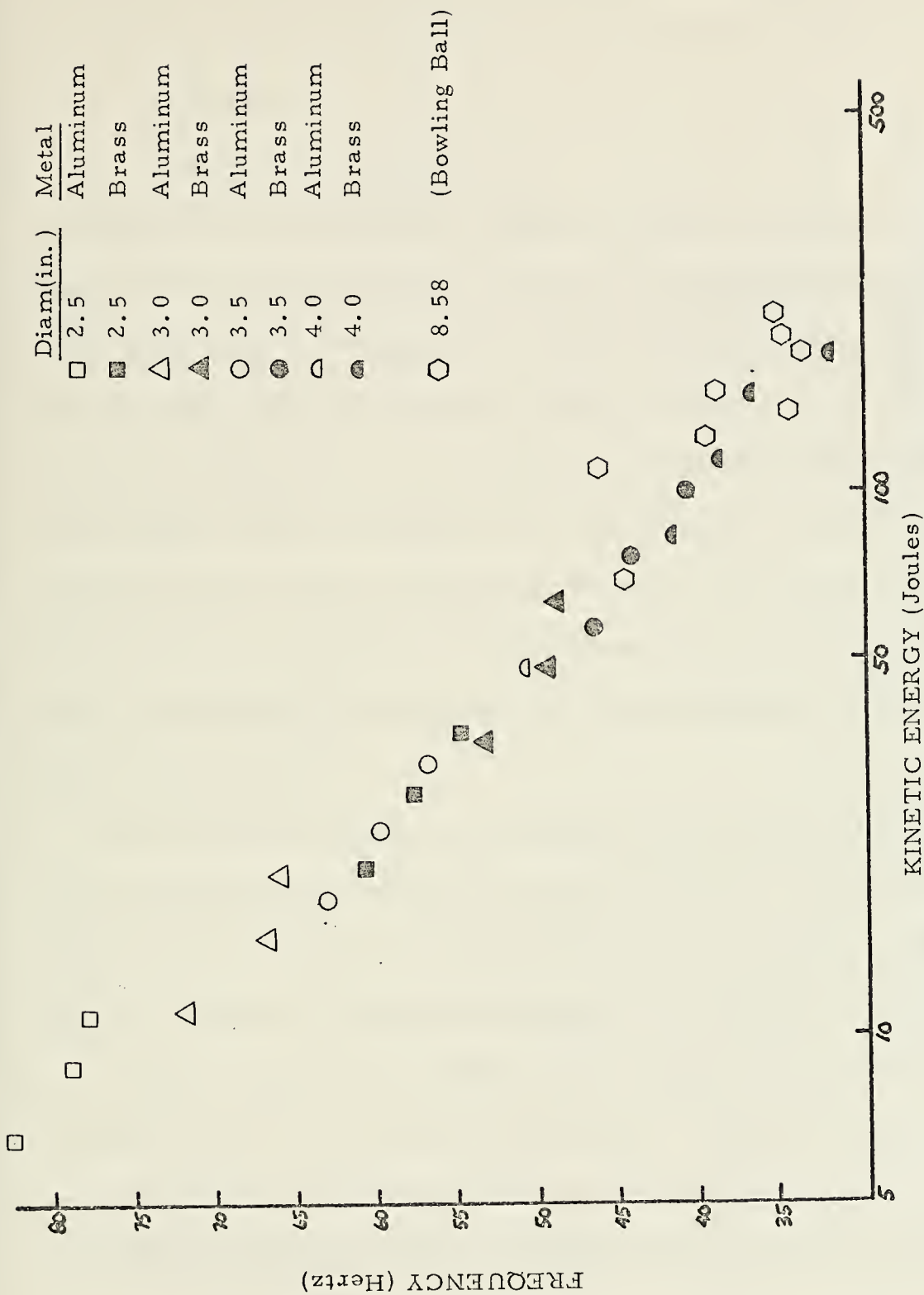


FIGURE 8. DOMINANT FREQUENCY vs. \log_{10} (IMPACTING KINETIC ENERGY)

For air at standard atmospheric pressure and assuming water density $\rho = 1.0 \text{ gm/cm}^3$, this expression simplifies to [6]:

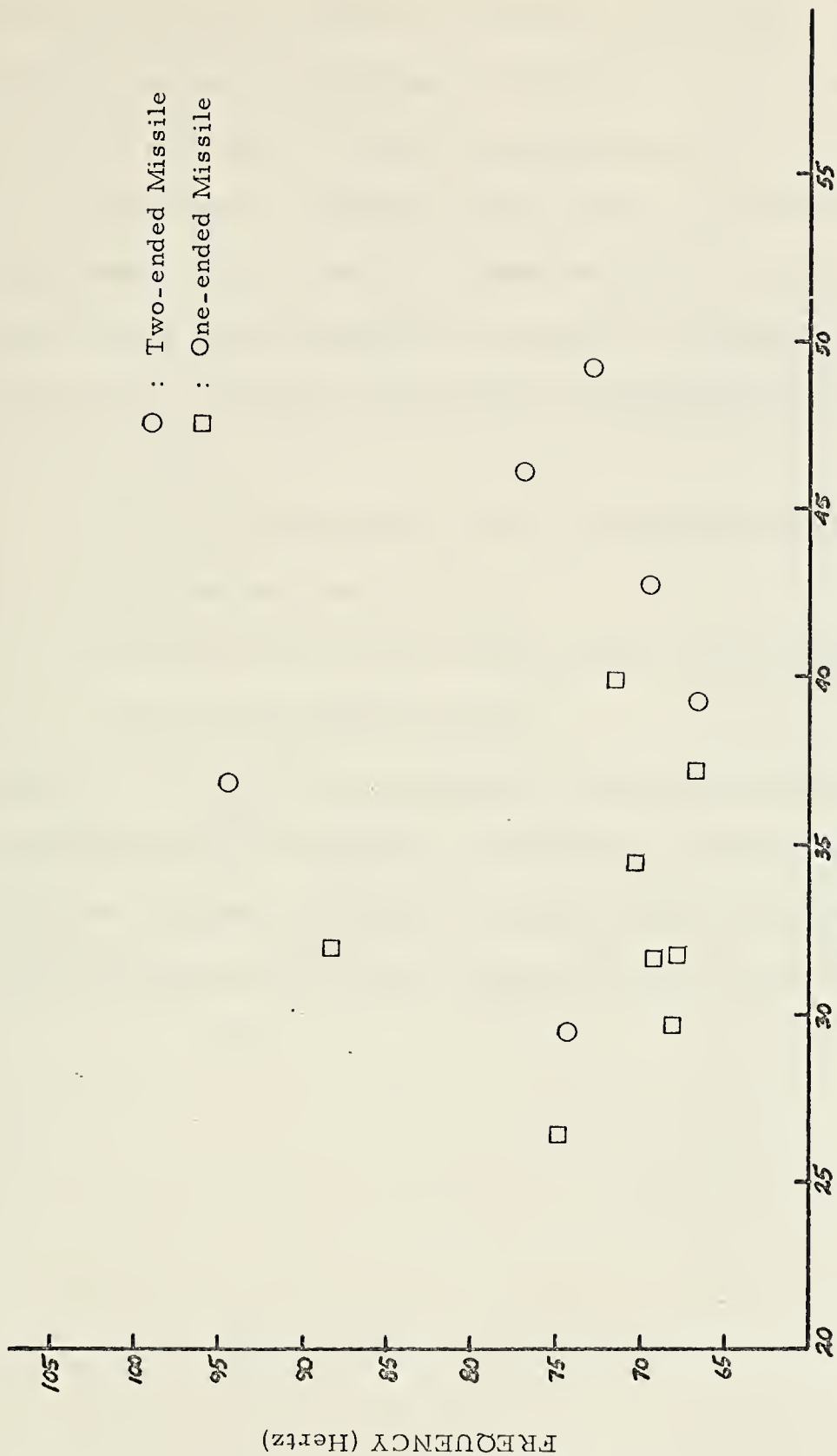
$$f = 328/a$$

where a is measured in cm.

In order to use this expression for any air cavity, the volume of the cavity must be known, and the radius of a volumetrically equivalent sphere determined. Although the quality of the movie film precluded an accurate measurement of cavity volume, the radius of the cavity's maximum cross-section was obtainable from the film frames, and on the average, values were within 25% of the calculated radius of a spherical cavity which would produce the measured frequency. This rough comparison provided an additional measure of confidence that the cavity pulsations were the source of the predominant segment of the recorded signal.

Data from the dropping of the bowling ball overlapped the data for the metal spheres and extended the curves of Figs. 7 and 8. The higher degree of scatter in the bowling ball data can be attributed to surface roughness and physical handling of the ball prior to drop.

Figure 9 presents the dominant signal frequency vs kinetic energy of impact for the missile-like shapes. While the limited range of energies obtainable and the scatter of the data make it difficult to say anything definite about these data, it is noteworthy that the signal frequencies of the streamlined bodies are significantly



KINETIC ENERGY (Joules)

FIGURE 9. MISSILE-LIKE SHAPES.

DOMINANT FREQUENCY vs. IMPACTING KINETIC ENERGY

greater than for the spheres of comparable impact kinetic energy. The two, higher frequency data were probably due to an observed change in attitude as the shapes transversed the cavity.

Figures 10 and 11 display the peak acoustic pressure at the hydrophone, Figs. 12 and 13 the signal energy flux density, and Figs. 14 and 15 the signal decay constant, all vs the kinetic energy of the body at impact. In all the plots, the following characteristics are observable:

1. For an individual body, some relationship between the plotted quantities is evident.
2. Collectively, the metal spheres show some interdependence between the plotted quantities.

However, it is apparent that if the plots of the metal spheres and the bowling ball were combined, the separation of the groups of data indicates that kinetic energy is not an appropriate parameter to relate the plotted quantities for a wide range of body sizes and masses.

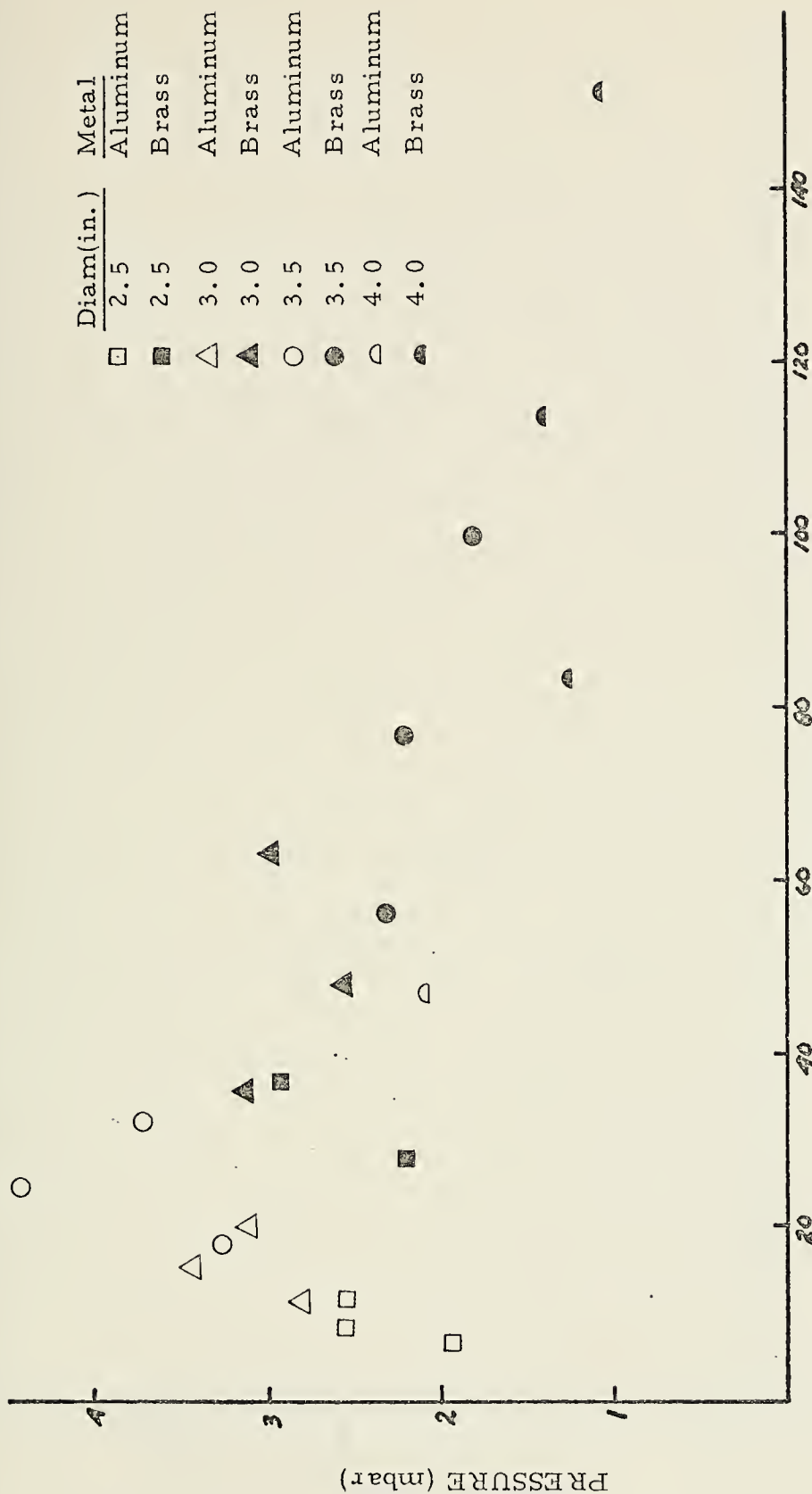
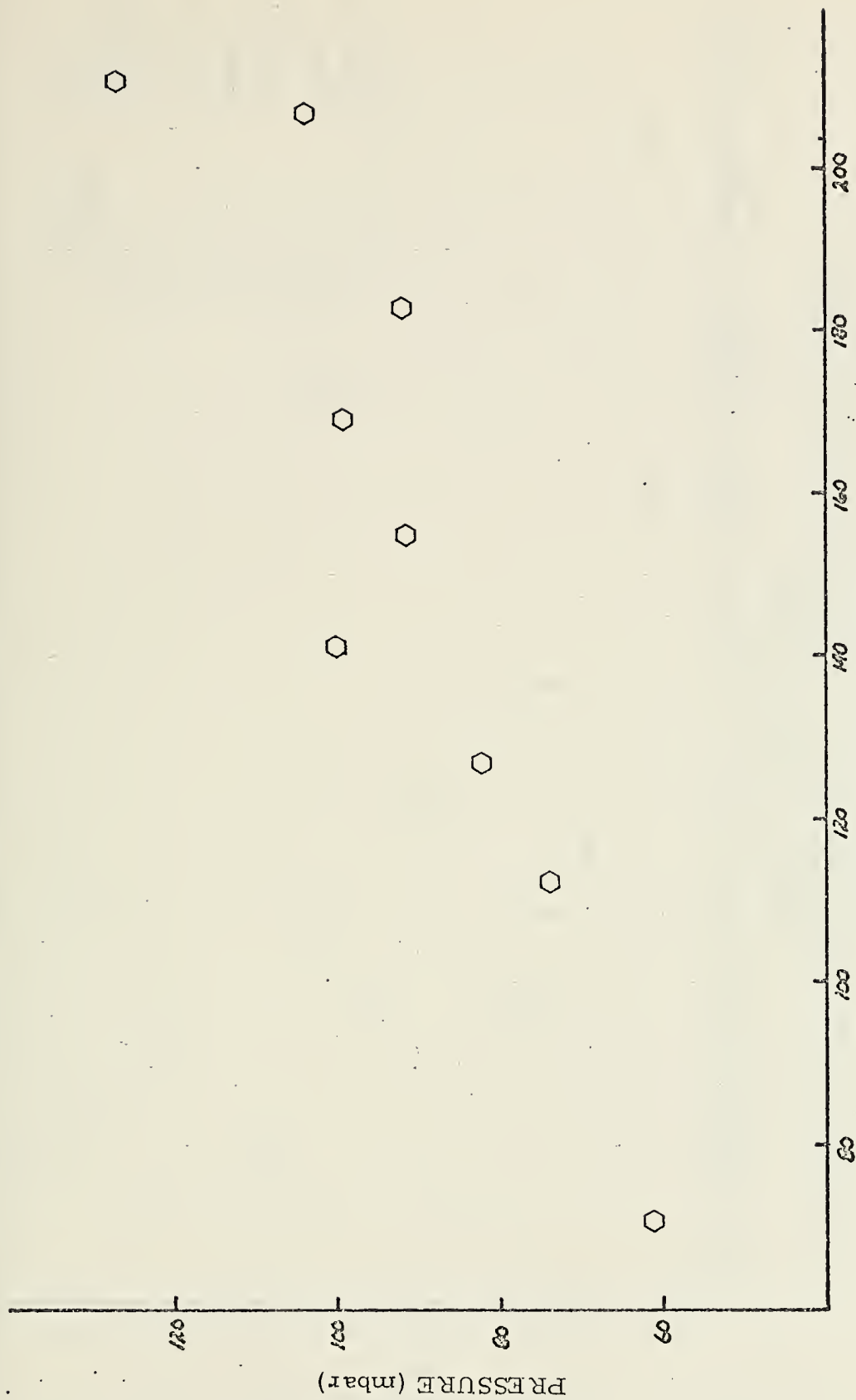
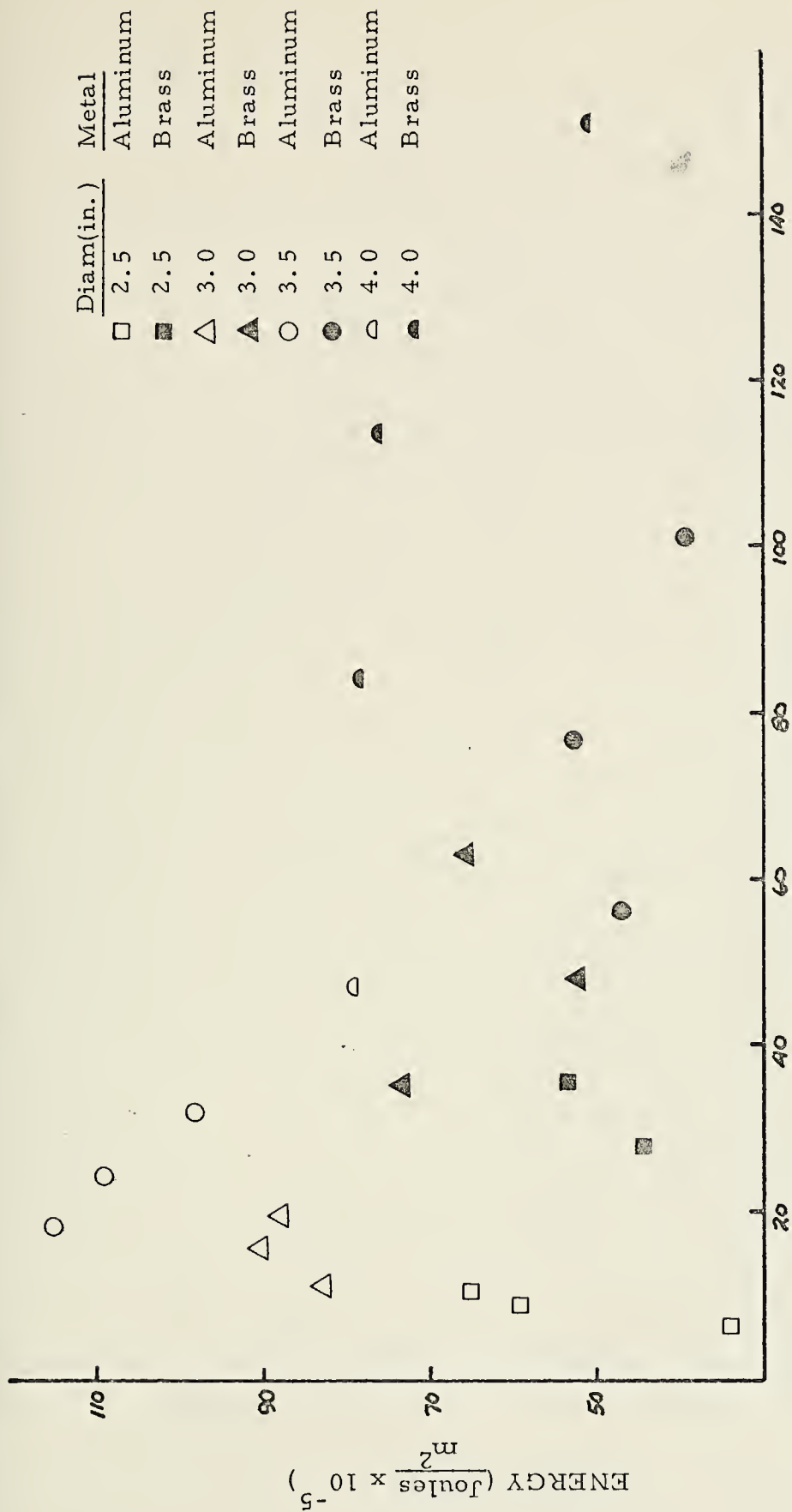


FIGURE 10. METAL SPHERES.
ACOUSTIC PRESSURE vs. IMPACTING KINETIC ENERGY



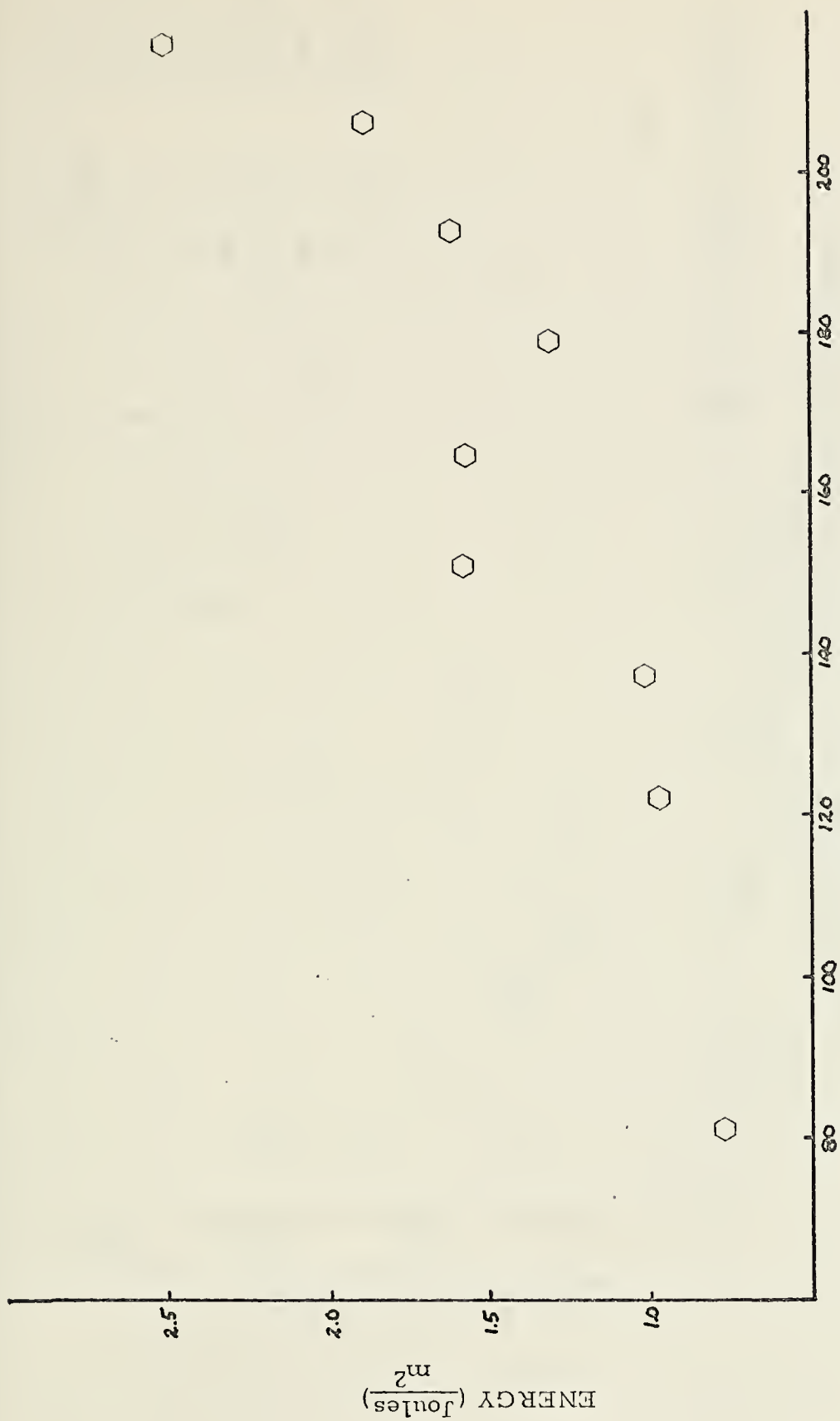
KINETIC ENERGY (Joules)
 FIGURE 11. BOWLING BALL
 ACOUSTIC PRESSURE vs. IMPACTING KINETIC ENERGY



KINETIC ENERGY (Joules)

FIGURE 12. METAL SPHERES.

ACOUSTIC ENERGY FLUX DENSITY vs. IMPACTING KINETIC ENERGY



KINETIC ENERGY (Joules)
 FIGURE 13. BOWLING BALL.
 ACOUSTIC ENERGY FLUX DENSITY vs. IMPACTING KINETIC ENERGY

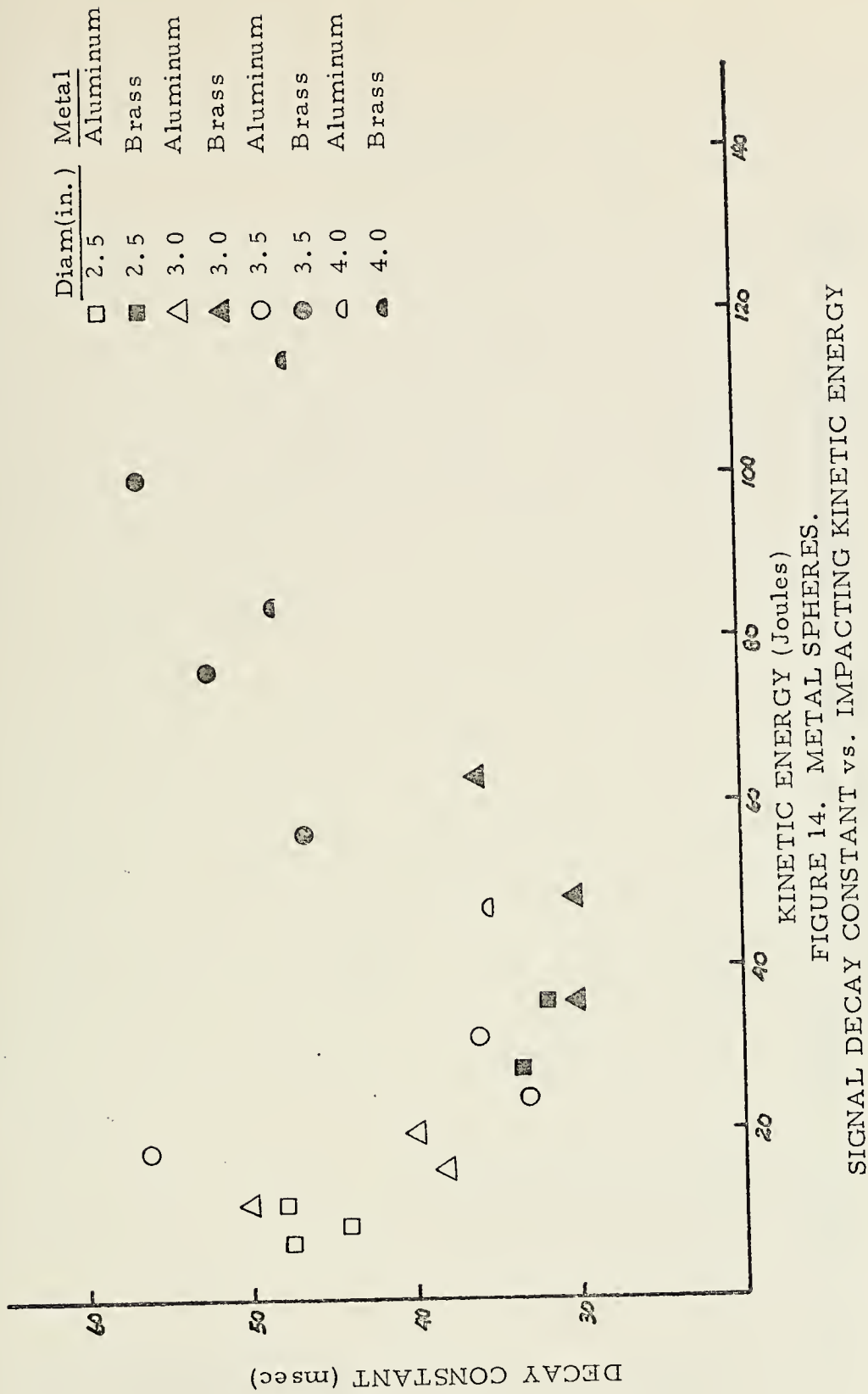
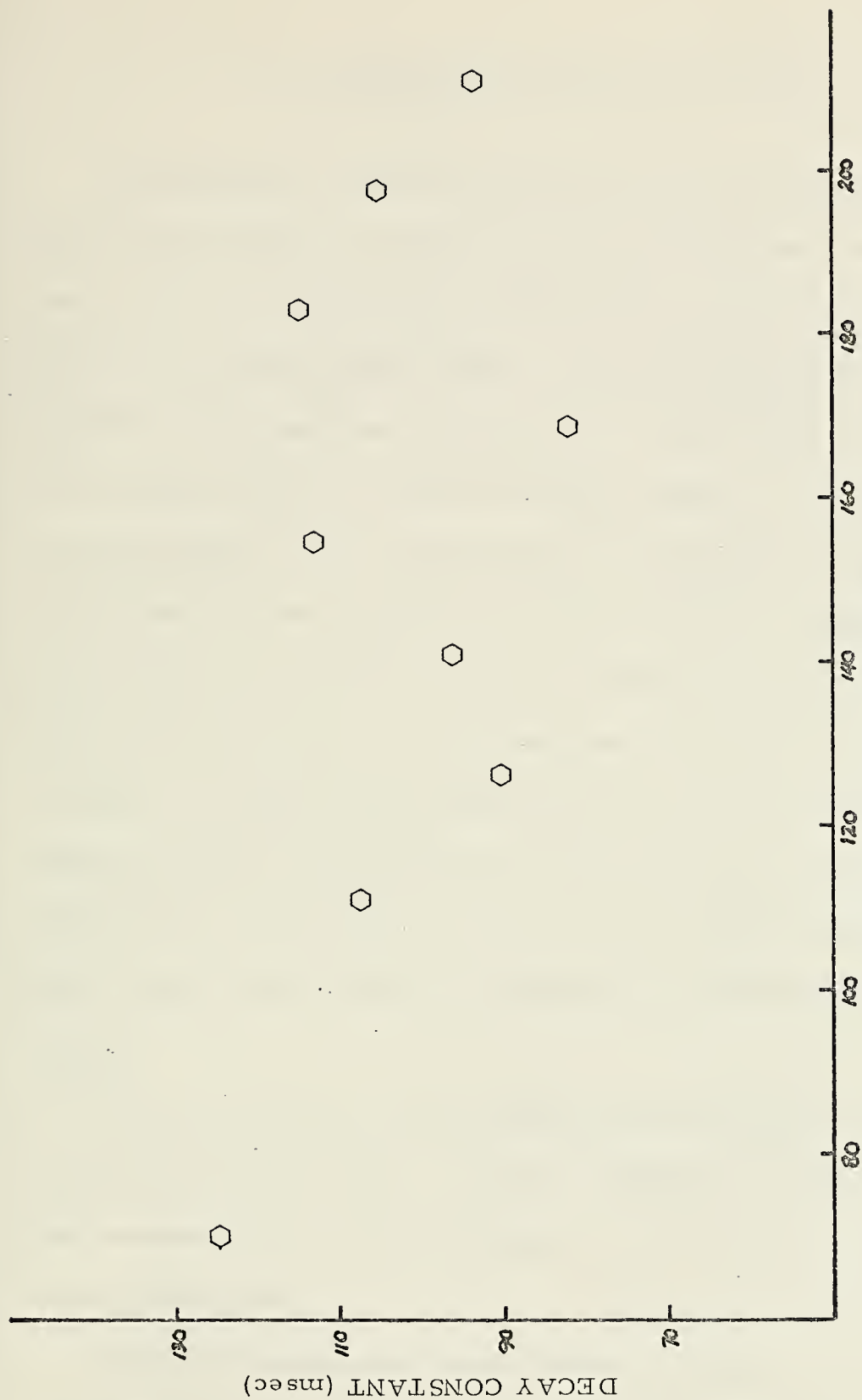


FIGURE 14. METAL SPHERES.
SIGNAL DECAY CONSTANT vs. IMPACTING KINETIC ENERGY



KINETIC ENERGY (Joules)

FIGURE 15. BOWLING BALL.

SIGNAL DECAY CONSTANT vs. IMPACTING KINETIC ENERGY

V. CONCLUSIONS AND APPLICATIONS

Undoubtedly the most important result of this research was the demonstration that, for a simple, spherical-shaped body, the dominant frequency resulting from the water entry correlates to the kinetic energy of the body at impact. It seems reasonable to believe that this relationship should also apply to a more complex-shaped body as long as the entry attitude remains constant. The significance of this frequency-energy relationship lies in the simplicity with which the dominant frequency emanating from the water entry signature for a given falling body can be predicted. Volumetric cavity measurements and conversion to an equivalent spherical cavity are not necessary. Rather, all one needs to know for a given body is its impacting kinetic energy and characteristic frequency-energy relationship. Conversely, the detection of a frequency resulting from a water entry provides an indication of the impacting kinetic energy.

The basic frequency-energy relationship has potential usefulness to a number of applications, and many of them are militarily oriented. The concepts of two possible applications are discussed in the subsequent paragraphs.

Consider the problem of knowing with some degree of accuracy the position of mines dropped into a minefield, assuming the mine

parameters of mass, impact velocity, and entry attitude are known. From experimental data, the approximate resultant frequency of the water entry would be known. Assume an array of passive listening devices is in place near this minefield. Knowledge of the frequency may provide the positive information that a mine has impacted, and in addition permits narrowing of the listening bandwidth yielding a higher signal-to-noise ratio. With properly placed listening devices, the position of impact could be fixed by the cross-bearing method.

During a tactical situation, the need may arise to identify a weapon as to its general type, i. e., bomb, torpedo, or mine. By knowing the general physical characteristics and the parameters for deployment, and by detecting the impacting signal of the weapon, an identification of the weapon could be made.

Determination of additional signature characteristics, particularly source level and directivity, would be of great value when considering the range to which a water entry signal can be detected. These areas were not pursued in this research but are suggested as possible extensions to what has been accomplished here. In addition, further research with non-spherical shapes might be considered, perhaps using scaled models of weapons, mines, sonobuoys, etc.

Body		Mass, kg	Height m	Velocity m/sec	Kinetic Energy j	Dominant Frequency Hz	Acoustic Pressure mbar	Acoustic Energy/cm ² x10 ⁻²	Decay Constant msec
diam(in.)	mat'l								
2.5	Alum.	0.364	3.265	8.0	11.63	78	2.540	64.5	48
2.5	Alum.	0.364	2.500	7.0	8.90	79	2.540	58.8	44
2.5	Alum.	0.364	1.837	6.0	6.54	83	1.905	34.5	47.5
2.5	Brass	1.147	3.265	8.0	36.65	55	2.820	52.9	32
2.5	Brass	1.147	2.500	7.0	28.05	58	2.325	44.1	33
2.5	Brass	1.147	1.837	6.0	20.61	61	--	--	--
3.0	Alum.	0.626	3.265	8.0	20.12	66	3.270	87.4	40
3.0	Alum.	0.626	2.500	7.0	15.43	67	3.445	89.5	36.5
3.0	Alum.	0.626	1.837	6.0	11.33	72	2.820	82.0	50.5
3.0	Brass	1.960	3.265	8.0	63.33	49	2.965	64.9	36
3.0	Brass	1.960	2.500	7.0	48.50	50	2.565	50.6	38
3.0	Brass	1.960	1.837	6.0	35.60	54	3.100	72.7	30
3.5	Alum.	0.995	3.265	8.0	31.95	57	3.665	108.1	36
3.5	Alum.	0.995	2.500	7.0	24.45	60	4.410	119.1	33
3.5	Alum.	0.995	1.837	6.0	17.95	63.5	3.245	124.8	56
3.5	Brass	3.140	3.265	8.0	100.50	41	1.800	37.75	56
3.5	Brass	3.140	2.500	7.0	77.00	44.5	2.200	52.05	52
3.5	Brass	3.140	1.837	6.0	56.50	47	2.310	46.5	46.5
4.0	Brass	4.68	3.950	8.8	181.50	32	--	--	--
4.0	Brass	4.68	3.265	8.0	151.30	37	1.090	50.0	93
4.0	Brass	4.68	2.500	7.0	114.50	39	1.395	75.7	74
4.0	Brass	4.68	1.837	6.0	84.10	42	1.267	77.7	76
4.0	Alum.	1.487	3.265	8.0	47.70	51	2.060	78.6	50

APPENDIX A. SUMMARY OF DATA

Body		Mass. kg	Height m	Velocity m/sec	Kinetic Energy j	Dominant Frequency Hz	Acoustic Pressure mbar	Acoustic Energy erg/cm ² x10 ⁻²	Decay Constant msec
diam(in.)	mat'l								
8.58	Bowl. B.	7.20	3.00	7.66	211.53	35.5	127.10	251000	94
8.58	Bowl. B.	7.20	2.80	7.40	197.43	35	104.00	187500	105
8.58	Bowl. B.	7.20	2.60	7.14	183.33	34	91.50	160000	115
8.58	Bowl. B.	7.20	2.40	6.85	169.23	37	99.00	132000	82
8.58	Bowl. B.	7.20	2.20	6.56	155.12	39	91.20	156500	113
8.58	Bowl. B.	7.20	2.00	6.26	141.02	35	99.60	157300	96
8.58	Bowl. B.	7.20	1.80	5.94	126.92	40	81.90	99700	90
8.58	Bowl. B.	7.20	1.60	5.60	112.82	46.5	73.50	96500	107
8.58	Bowl. B.	7.20	1.00	4.43	70.51	45	61.20	78000	124

APPENDIX A. SUMMARY OF DATA

Missile Shape no. tapered ends	Mass kg	Height m	Velocity m/sec	Kinetic Energy j	Dominant Frequency Hz
One	1.353	3.00	7.66	39.80	71.5
One	1.353	2.80	7.40	37.15	66.5
One	1.353	2.60	7.14	34.50	70
One	1.353	2.40	6.85	31.80	68
One	1.353	2.20	6.56	29.80	68
One	1.353	2.00	6.26	26.50	74.5
Two	1.670	3.00	7.66	49.10	73
Two	1.670	2.80	7.40	45.80	77
Two	1.670	2.60	7.14	42.60	69.5
Two	1.670	2.40	6.85	39.30	66.5
Two	1.670	2.20	6.56	36.75	94
Two	1.670	1.80	5.94	29.50	74

APPENDIX A. SUMMARY OF DATA

BIBLIOGRAPHY

1. Alden Research Laboratories Report 115-72/SP, Water Entry, by A. May, September 1972.
2. A. M. Worthington, "On the Forms Assumed by Drops of Liquid Falling Vertically on a Horizontal Plate," Royal Society of London Proceedings, v. 25, p. 261-271, 1877.
3. A. M. Worthington, "On Impact with a Liquid Surface," Royal Society of London Proceedings, v. 34, p. 217-230, 1882.
4. A. M. Worthington and R. S. Cole, "Impact with a Liquid Surface, Studied by the Aid of Instantaneous Photography," Philosophical Transactions, v. 189A, p. 137-148, 1897.
5. A. M. Worthington and R. S. Cole, "Impact with a Liquid Surface Studied by the Aid of Instantaneous Photography," Transactions of the Royal Society, v. 194A, p. 175-199, 1899.
6. M. Minnaert, "On Musical Air-Bubbles and the Sounds of Running Water," Philosophical Magazine, v. 16, p. 235-248, 1933.
7. David Taylor Model Basin Report C-595, The Underwater Sound from the Splashes of Water Droplets, by G. J. Franz, January 1955.
8. A. May and J. Woodhull, "Drag Coefficients of Steel Spheres Entering Water Vertically," Journal of Applied Physics, v. 19, p. 1109-1121, 1948.
9. A. May, "Effect of Surface Condition of a Sphere on Its Water-Entry Cavity," Journal of Applied Physics, v. 22, p. 1219-1222, 1951.
10. A. May, "Vertical Entry of Missiles into Water," Journal of Applied Physics, v. 23, p. 1362-1372, 1952.
11. E. G. Richardson, "The Impact of a Solid on a Liquid Surface," Proceedings of the Physical Society (London), v. 61, p. 352-367, 1948.

12. E. G. Richardson, "The Sounds of Impact of a Solid on a Liquid Surface," Proceedings of the Physical Society (London), v. 68, p. 541-547, 1955.
13. G. J. Franz, "Splashes as Sources of Sound in Liquids," Journal of the Acoustical Society of America, v. 31-8, p. 1080-1096, August 1959.
14. Kay Electric Company Instruction Manual, Missilyzer Missile Data-Reduction Spectrograph.
15. EMR Telemetry, Weston Instruments, Inc. Specification, Model 1510 Spectrameter, 1973.
16. Precision Instrument Company Instruction Manual, Portable Instrumentation Tape Recorder Model PI-6200, August 1967.

INITIAL DISTRIBUTION LIST

	No. Copies
1. Defense Documentation Center Cameron Station Alexandria, Virginia 22314	2
2. Library, Code 0212 Naval Postgraduate School Monterey, California 93940	2
3. Assoc. Professor J. V. Sanders, Code 61Sd Department of Physics and Chemistry Naval Postgraduate School Monterey, California 93940	1
4. Dr. Victor Dawson, Code 322 Hydroballistics and Mechanics Section Building 427, Room 438 Naval Ordnance Laboratory White Oak, Maryland 20910	1
5. LT Brian Douglas Uber, USN 1 Marlyn Street Bridgeton, New Jersey 08302	1
6. LCDR Robert Joseph Fegan, Jr., USN Operational Test and Evaluation Force Naval Base Norfolk, Virginia 23511	1

SECURITY CLASSIFICATION OF THIS PAGE (When Data Entered)

DD FORM 1 JAN 73 1473 EDITION OF 1 NOV 65 IS OBSOLETE
(Page 1) S/N 0102-014-6601 | 50
Unclassified
SECURITY CLASSIFICATION OF THIS PAGE (When Data Entered)

20.

The oscillation of the air-filled cavity behind the bodies after impact was found to produce the most predominant aspect of the acoustic signature and the resultant frequency of these oscillations was dependent upon the impacting kinetic energy and shape of the body. Other signal characteristics investigated were total acoustic energy, peak acoustic pressure, and decay rate but correlation with the parameters of the bodies was not obvious.

Thesis
U125
c.1

Uber

Acoustic signatures
accompanying low-velo-
city water entry.

147562

Thesis
U125
c.1

Uber

Acoustic signatures
accompanying low-velo-
city water entry.

147562

thesU125

Acoustic signatures accompanying low-vel



3 2768 001 88926 4

DUDLEY KNOX LIBRARY